ELSEVIER

Journal of Alloys and Compounds 419 (2006) 98–102

Journal of ALLOYS AND COMPOUNDS

www.elsevier.com/locate/jallcom

The mechanical properties of Al_2O_3/aluminum alloy A356 composite manufactured by squeeze casting

Shang-Nan Chou [a], Jow-Lay Huang [a,*], Ding-Fwu Lii [b], Horng-Hwa Lu [c]

[a] *Department of Material Science and Engineering, National Cheng-Kung University, Tainan 701, Taiwan, ROC*
[b] *Department of Electrical Engineering, Cheng Shiu Institute of Technology, Kaohsiung County, Taiwan 833, Taiwan, ROC*
[c] *Department of Mechanical Engineering, National Chin-Yi Institute of Technology, Taiping, Taichung 411, Taiwan, ROC*

Received 6 May 2005; received in revised form 1 October 2005; accepted 4 October 2005
Available online 14 November 2005

Abstract

Porous aluminum oxide (Al_2O_3) preforms were formed by sintering in air at 1200 °C for 2 h. The A356 aluminum alloy was infiltrated into the preforms in order to fabricate Al_2O_3/A356 composites with different volume content of A356 by squeeze casting. The volume contents of A356 alloy in Al_2O_3/A356 composites were 5–40 vol.%. For the corresponding composites, the four-point bending strength of the composites changed from 397 to 443 MPa, the hardness decreased from 1109 to 227 HV and the fracture toughness increased from 4.97 to 11.35 MPa $m^{1/2}$. One can fine three toughening mechanisms, crack bridging, crack deflection and crack branching in the composites on SEM micrograph.

Keywords: Al_2O_3/A356 composites; Squeeze casting; Infiltration; Four-point bending strength; Hardness; Toughness

1. Introduction

Aluminum oxide (Al_2O_3) is a hard refractory ceramic, which has been investigated for high temperature structural and substrate applications because of its good strength and low thermal expansion coefficient. Nevertheless, like other monolithic ceramics, Al_2O_3 is apt to suffer from low ductility and low fracture toughness. Therefore, metals (e.g. aluminum, cobalt, niobium) or alloys were added to ceramics for the purpose of improving their toughness [1–5].

Recently, the demands for lightweight materials having high strength and high toughness have attracted much attention in the development of ceramic-matrix composites (CMCs). CMCs represent a new class of materials, which are on their way to substitute conventional materials in many fields. In the last few years, considerable advances have been made in the development of manufacturing processes for CMCs, which have led to higher damage tolerance and reduction in weight [6]. The most important limitation of the fabrication of CMCs by liquid-phase process relies on the compatibility of the reinforcement and the matrix [7]. This problem is especially important in the case of aluminum matrix composites, because aluminum is usually covered with a thin oxide layer which blocks surface wetting. Several methods have been investigated to improve the compatibility at the interface [8–11]. The squeeze casting is one of the most favorable processes, since the contact time between the reinforcement and the aluminum melt is short [12,13].

In this study, porous Al_2O_3 preforms were formed by sintering in air at 1200 °C for 2 h. Molten aluminum alloy was infiltrated into the preforms to make Al_2O_3/A356 composite by squeeze casting. The physical and mechanical properties of the composite were measured. The effects of the composition on the physical and mechanical properties have also been investigated. In addition, the microstructure and fracture behavior of the composites were examined.

2. Experimental

2.1. Sample preparation

The second phase to improve strength and toughness of Al_2O_3 ceramic matrix in this study was aluminum alloy A356, the composition is shown in Table 1. The Al_2O_3 powders were extracted from thermally reactive process (A16SG ALCOA, USA), the particle size being about 0.3–0.5 μm. The structure of Al_2O_3 powders are α-phase, with purity higher than 99.8%.

The Al_2O_3 powders were first mixed homogeneously with 5, 10, 20, 30 and 40 vol.% of paraffin wax at 80 °C. The mixture was then placed in a stainless

* Corresponding author. Tel.: +886 6 2348188; fax: +886 6 2763586.
E-mail address: jlh888@mail.ncku.edu.tw (J.-L. Huang).

0925-8388/$ – see front matter © 2005 Elsevier B.V. All rights reserved.
doi:10.1016/j.jallcom.2005.10.006

Table 1
The chemical composition of A356 alloy

Elements	Content (wt.%)
Si	7.13
Mg	0.63
Fe	0.11
Cu	<0.1
Zn	0.07
Al	Rest

steel die to exert 20 MPa pressure to form the Al_2O_3 preform. Then they were thermally debinded at 300 °C for 2 h to remove paraffin wax and sintered in air at 1200 °C for 2 h. The porous Al_2O_3 preforms with different pore content of 5, 10, 20, 30 and 40 vol.% were then made. The molten aluminum alloy A356 was infiltrated into the preform to form Al_2O_3/A356 composite. The apparatus and processes of squeeze casting are shown schematically in Fig. 1. The squeeze casting processes included four steps: (1) preheating the casting die to 600 °C, and preparing molten A356 alloy; (2) Al_2O_3 preform setting (preheated in furnace to 600 °C); (3) high mechanical pressure for infiltration and (4) release the pressure and extraction of the ingot [14]. During the squeeze casting process, the downward velocity of squeeze head was 0.8–5 cm/s with a pressure of 200 MPa, and the loading time at high pressure was 30 s.

The composites were then cut and polished to 1 μm. Because the apparent difference between ceramic and aluminum alloy phases, the Al_2O_3/A356 composites were not etched for scanning electron microscopy (SEM). The density and mechanical properties of the composites were measured. The effects of the composition on the physical and mechanical properties were investigated. In addition, the microstructure and fracture behavior of the composite were examined.

2.2. Density and mechanical properties

The density was measured by the water displacement technique. The hardness was determined applying a Vickers (Akashi AVK C21) indenter and calculated as $H = P/2d^2$, where d is the half-diagonal indentation impression and P is the indentation load (196 N for 15 s). Flexural strength was measured by a four-point bending test on an Instron universal testing machine (series 8511, Instron Co., Canton, MA, USA). The outer and inner spans were 40 and 20 mm, respectively. The nominal dimensions of the testing bars were 3 mm × 4 mm × 50 mm. Fracture toughness was measured in the same testing fixture using a single edge notched beam (SENB) method [15,16]. The maximum test load and the moment of the four-points bending load were used to calculate the toughness of the composite according to the following equation:

$$K_{IC} = \frac{6Ma^{1/2}}{db^2}Y$$

with:

$$M = \left(\frac{P}{2}\right)\frac{(L_1 - L_2)}{2}$$

$$Y = 1.99 - 2.74\left(\frac{a}{b}\right) + 12.97\left(\frac{a}{b}\right)^2 - 23.17\left(\frac{a}{b}\right)^3 + 24.80\left(\frac{a}{b}\right)^4$$

where P is the maximum test load, M the moment of the four-points bending load, d and b the width and height of the bending samples bar, respectively, a the depth of the single edge notched, L_1 and L_2 the outer and inner spans, respectively, and Y is the equation about (a/b) ratio. For the stable crack growth mode in the single edge notched beam four-point bending specimen, it was suggested that $a/b = 1/2$, $L_1 = 40$ mm and $L_2 = 20$ mm.

2.3. Microstructural analysis

The phases of the as-received Al_2O_3/A356 composites were analyzed by an X-ray diffractometer (Rigaku D/Max-II BX) using Cu Kα radiation (30 KV, 20 mA) in the range of 20–80° at a speed of 4°/min. The polished specimens of the composite were observed and characterized using optical microscope (OM) and image analyzer (Optimas, Vol. 1.0, Imaging Fundamentals, Tacoma, WA). Each image is divided into nine discrete elements (pixels), and entered into a digital computer to calculate the volume fraction of Al_2O_3/A356 composite. Fracture surfaces and crack propagation behavior were scrutinized using OM and scanning electron microscopy (SEM, Hitachi S-4200). Etching is not necessary for optical micro-structural examination due to the adequate contrast between the bright A356 and dark Al_2O_3.

3. Results and discussions

3.1. Phase analysis

The X-ray diffraction patterns of A356 alloy, Al_2O_3 powder, Al_2O_3 preform, and Al_2O_3/A356 composite are shown in Fig. 2. Fig. 2d shows that the Al_2O_3/A356 composite consists only of α-Al_2O_3 ceramic and A356 alloy. Because of the stability of α-Al_2O_3 against molten Al-alloys, is a hard refractory ceramic to reaction at high temperature, one can not find any other reaction product in the compositions.

3.2. Compositional and micro-structural analysis

The Al_2O_3/A356 composites made from Al_2O_3 preforms at five A356 volume contents (5, 10, 20, 30 and 40%) were designated as Al5, Al10, Al20, Al30 and Al40, respectively.

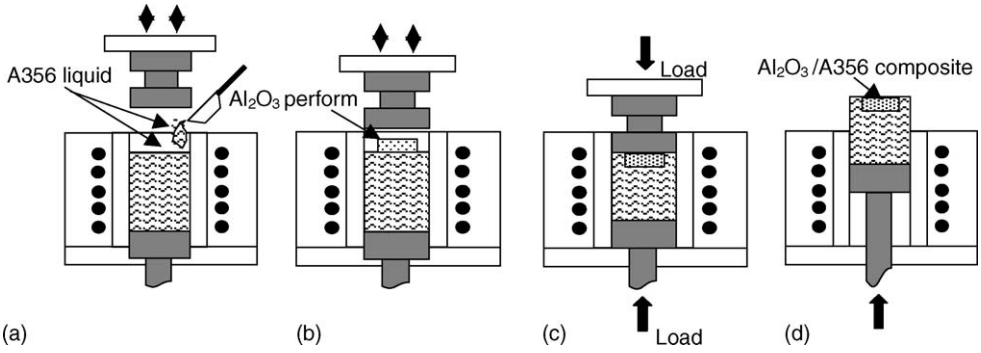

Fig. 1. Schematic of the squeeze-casting process: (a) flow of A356 liquid into the mold, (b) placing of the Al_2O_3 preform into the mould, (c) application of pressure (200 MPa) for infiltration, (d) pressure release and extraction of the ingot.

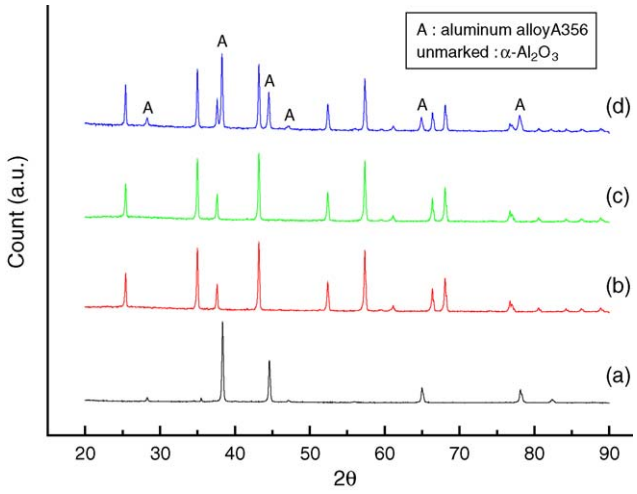

Fig. 2. X-ray diffraction patterns of: (a) A356 aluminum alloy, (b) Al_2O_3 powder, (c) Al_2O_3 preform, (d) Al_2O_3/A356 composite.

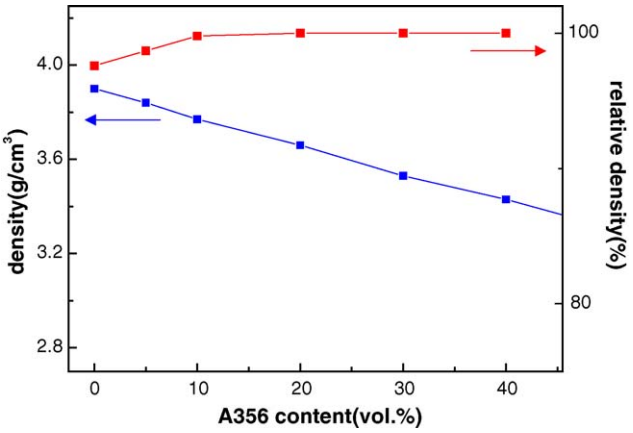

Fig. 4. The density and relative density versus aluminum alloy A356 content in Al_2O_3/A356 composites.

A typical optical photograph showing the microstructure of the Al_2O_3/A356 composite (Al10) is shown in Fig. 3a, and in Fig. 3b as TEM bright field image. These two pictures show that the Al_2O_3/A356 composite has a uniform distribution between and the ceramic phase and alloy phase. Because the A356 alloy contains elementary silicon and high mechanical pressure to exert upon the composites during squeeze casting process.

3.3. Density measurement

The Al_2O_3/A356 composites fabricated in this study contain 5–40 vol.% aluminum alloy A356. The density of A356 is 2.713 g/cm^3, and the density of α-Al_2O_3 is 3.987 g/cm^3. The tendency of density change was shown in Fig. 4. The density decreases with increasing A356 content from 5 to 40 vol.% in a linear mode, and the relative density of composites fabricated with squeeze casting with a high mechanical pressure of 200 MPa for 30 s were almost 100%.

3.4. Mechanical properties

3.4.1. Hardness

The results of hardness measurements are shown in Fig. 5. The hardness decreased dramatically from 1009 to 227 HV by increasing the A356 from 5 to 40 vol.%. This is because the A356 alloy is a comparable soft material. The hardness of pure Al_2O_3 and pure A356 Al-alloy are 1800 HV and 70 HB, respectively. One can get the hardness of CMCs decreases with increasing A356 Al-alloy contents from 5 to 40 vol.%.

3.4.2. Bending strength

Fig. 6 shows the four-points bending strength relating to different A356 contents of the Al_2O_3/A356 composites. The four-points bending strength of the composites increased from 397 to 482.5 MPa with increasing the A356 contents from 0 to 10 vol.%, and then decreased from 482.5 to 443 MPa with further increasing the A356 contents to 40 vol.%. It is because the relative density increases from 97.5 to about 100% (Fig. 4). Nevertheless, the strength decreases with increasing A356 content

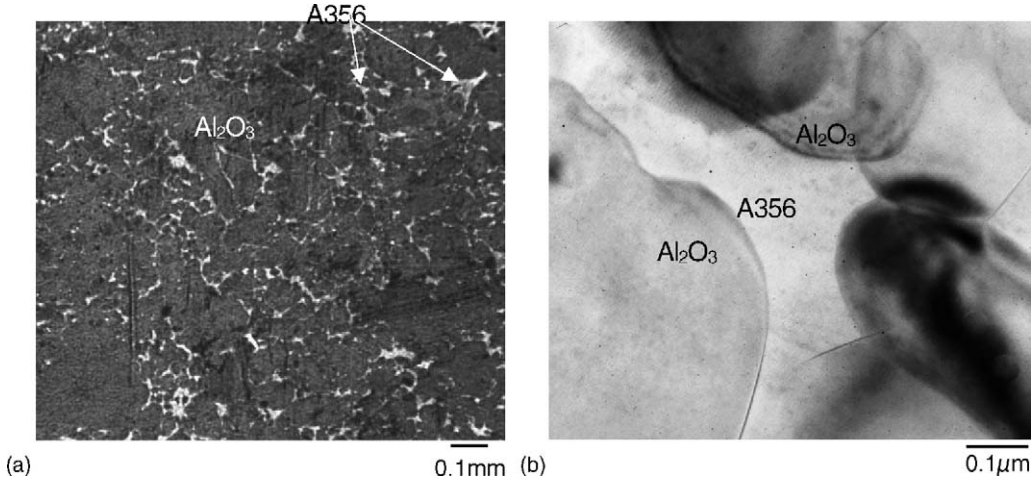

Fig. 3. Micro-photographs showing the microstructure of Al_2O_3/A356 composite (Al10): (a) optical photograph, the bright area is A356 and the dark area is Al_2O_3, (b) TEM micro-photograph, showing that the paraffin wax appearing as connected path.

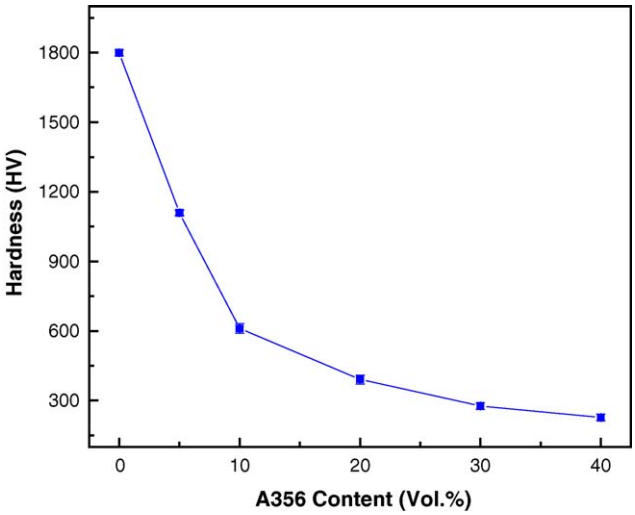

Fig. 5. Vickers hardness vs. aluminum alloy A356 content in Al_2O_3/A356 composites.

from 10 to 40 vol.%, but the relative densities were the same to approach 100%; the strength decreases because the materials were infiltrated with the soft material aluminum alloy A356.

3.4.3. Fracture toughness and toughening mechanisms

Fig. 7 shows the fracture toughness of the Al_2O_3/A356 composites with different contents of A356. The fracture toughness increased from 4.97 to 11.35 MPa $m^{1/2}$ with increasing A356 content from 5 to 40 vol.%. The fracture toughness of all of these composites were higher than pure ceramic material, Al_2O_3. Because we infiltrated a high fracture toughness material, aluminum alloy A356, the fracture toughness increased with increasing A356 content.

One can find crack bridging, crack deflection and crack branching in the composites in the SEM micrograph. These three conditions are the toughening mechanism shown in Fig. 8. Fracture toughness means the capability to prevent and stop crack growth, typically relying on these three toughening mechanisms [17–19]: crack bridging, crack deflection and crack branching,

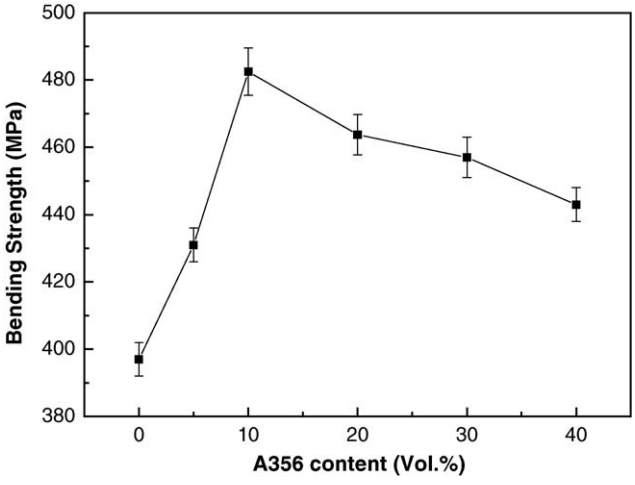

Fig. 6. Bending strength vs. aluminum alloy A356 contents in Al_2O_3/A356 composites.

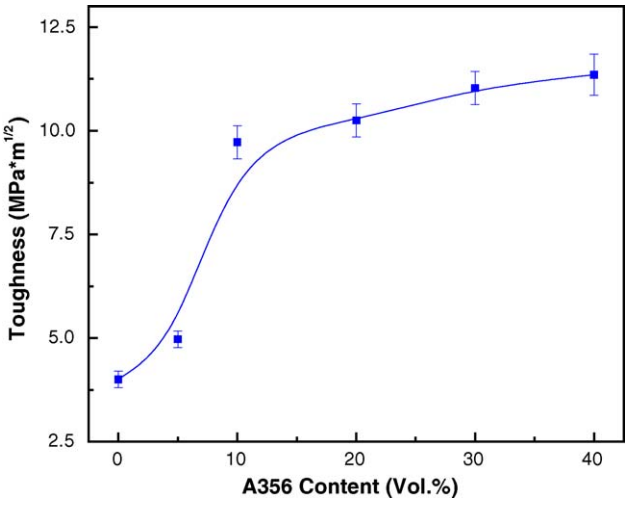

Fig. 7. Fracture toughness vs. aluminum alloy A356 contents in Al_2O_3/A356 composites.

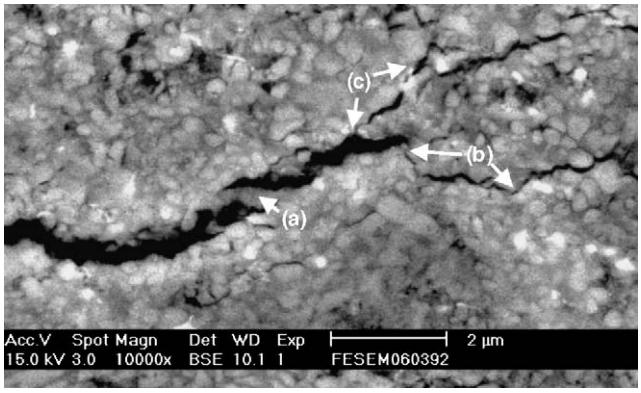

Fig. 8. Three toughening mechanisms: (a) crack bridging, (b) crack deflection, and (c) crack branching in Al_2O_3/A356 composites.

to scatter and disappear the energy of cracks growth, and then prevent and stop cracks growth. Crack bridging (Fig. 8a arrow area) was almost leading by soft materials of composite, aluminum alloy A356. Crack deflection (Fig. 8b arrow area) can scatter and dissipate the energy of cracks by increasing the crack length and make the crack turn. Crack branching (Fig. 8c arrow area) was also increasing the crack length from major crack to several minor cracks.

4. Conclusion

1. The density decreases linearly with increasing A356 content from 5 to 40 vol.%, and the relative densities of all composites were almost 100%.
2. As the A356 content increased from 5 to 40 vol.%, the hardness decreased substantially from 1009 to 227 HV. With increasing the A356 contents from 5 to 40 vol.%, the fracture strength decreased from 492.5 to 457 MPa.
3. The four-points bending strength of the composites increased from 397 to 482.5 MPa with increasing the A356 contents from 0 to 10 vol.%, but decreased from 482.5 to 443 MPa with increasing the A356 contents from 10 to 40 vol.%.

4. The fracture toughness increased from 4.97 to 11.35 MPa $m^{1/2}$ with increasing A356 content from 5 to 40 vol.%.
5. One can fine three toughening mechanisms, crack bridging, crack deflection and crack branching in the composites on SEM micrograph.

Acknowledgment

The authors would like to thank National Science Council of the Republic of China for its financial support under the Contract No. NSC-91-2622-E-006-061-CC3.

References

[1] C. Toy, W.D. Scott, J. Am. Ceram. Soc. 73 (1) (1990) 97–101.
[2] B.D. Flinn, M. Ruhle, A.G. Evans, Acta Metall. 37 (11) (1989) 3001–3006.
[3] D.C. Halverson, A.J. Pyzik, I.A. Aksay, W.E. Snowden, J. Am. Ceram. Soc. 72 (5) (1988) 775–780.
[4] L.S. Sigl, H.F. Fischmeister, Acta Metall. 36 (4) (1988) 887–897.
[5] L. Shaw, R. Abbaschian, J. Mater. Sci. 30 (1995) 849–854.
[6] A.G. Evans, R. Naslain (Eds.), Ceramic Transaction 58, The American Ceramic Society, 1995.
[7] A. Alonso, A. Paamies, et al., Metall. Trans. 24A (1993) 1423.
[8] R. Smith, F.H. Fores, J. Metall. (1992) 85.
[9] Shy-Wen Lai, D.D.L. Chung, J. Mater. Sci. 29 (1994) 3128–3150.
[10] P.K. Rohtagi, D. Nath, S.S. Singh, B.N. Keshavaram, J. Mater. Sci. 129 (1994) 5970.
[11] A.-B. Ma, H. Gan, T. Imura, Y. Nishida, J.-Q. Jiang, M. Takagi, Mater Trans. 38 (9) (1997) 812–816.
[12] S. Chu, R. Wu, Comp. Sci. Technol. 59 (1999) 157–162.
[13] A.M. Assar, M.A. Al-Nimir, J. Comp. Mater. 28 (1994) 1480.
[14] Ding-Fwu Lii, Jow-Lay Huang, Shao-Ting Chang, J. Eur. Ceram. Soc. 22 (2002) 253–261.
[15] G.K. Bansal, W.H. Duckworth, in: S.W. Freiman (Ed.), Fracture Mechanics Applied to Brittle Materials, STP 678, ASTM, 1973, p. 38.
[16] R.F. Pabsi, in: R.C. Bradt, D.P.H. Hasselman, F.F. Lange (Eds.), Fracture Mechanics of Ceramics: Microstructure, Materials, and Applications, vol. 2, Plenum Press, 1974, p. 555.
[17] A.G. Evans, in: J.A. Pask, A.G. Evans (Eds.), Ceramic Microstructures '86, Plenum Press, 1987, p. 775.
[18] R.W. Rice, Ceram. Eng. Sci. Proc. 6 (7–8) (1985) 589.
[19] R.W. Steinbrech, J. Eur. Ceram. Soc. 10 (1992) 131.